APPLICATIONS OF NETWORKED UNMANNED AERIAL VEHICLES TO COOPERATIVE FIRE DETECTION USING GRID-BASED DATA FUSION TECHNIQUES [1]

Luis Merino * **Fernando Caballero** **
Aníbal Ollero **
Robotics, Vision and Intelligent Control Group

* *Pablo de Olavide University, Seville, Spain,*
lmercab@upo.es
** *University of Seville, Seville, Spain*
{*caba,aollero*}*@cartuja.us.es*

Abstract: The paper presents a system for cooperative fire detection by means of a fleet of networked heterogeneous UAVs. A grid is used to represent the probability of having fire in a certain position within a given area. Different sensors are considered: infrared and visual cameras and a specialized fire sensor. A Bayesian approach is followed for the integration of the sensor readings and the evolution of the grid as new information is available. The paper presents results from actual field experiments of small controlled fires.

Keywords: Cooperative perception, grid-based data fusion, networked robots, aerial robotic vehicles

1. INTRODUCTION

Multi-robot teams have been object of research during the last decade. Recently, research results on teams of Unmanned Aerial Vehicles (UAVs) have been presented (Ollero *et al.*, 2005).

Cooperative perception is a main issue for networked robot teams. We could define cooperative perception as the collaboration between the networked robots for the estimation of the state of the environment, by sharing information or even by developing cooperative actions.

Data fusion procedures are needed to take advantage of the presence of several information sources. Moreover, in a team of heterogeneous UAVs, the vehicles will carry sensors of different nature, due to their different characteristics in terms of payload and others. Therefore, the fusion algorithms have to cope with different kinds of information.

Grids have been widely used as a method for single and multi-robot localization and mapping tasks (Thrun, 2001), and also for data fusion (Stepan *et al.*, 2005). This paper presents a grid-based data fusion algorithm for multi-UAV cooperative fire detection. The algorithm considers different types of data (images of different modalities and fire detector readings). A Bayesian approach is used to compute the evolution of the grid each time new data are available. This approach does not need explicit data association, being more robust than other methods that require the notion of contacts. Although the techniques are applied for fire detection, the same scheme can be used for other applications.

[1] Partially supported by the European Commission (COMETS IST-2001-34304) and the Spanish Government (AEROSENS DPI2005-02293)

Fig. 1. Two UAVs looking for a fire.

The paper presents results from field experiments, in which the objective is that a group of networked UAVs search a given area looking for fire alarms. If a potential alarm(s) is detected, the fleet should confirm or discard it, taking benefit of the diversity of sensors. The fleet should also provide the geographical position of the alarm. Each step implies some replanning mechanism and usually involves new paths for the robots. Figure 1 shows a photography of these experiments.

The rest of the paper is organized as follows. Section 2 presents the sensors considered and the preprocessing applied over the raw data. Section 3 describes the grid-based data fusion algorithm. Finally, Section 4 presents results from the field experiments.

2. SENSORS AND PREPROCESSING

The fleet considered in this paper is heterogeneous in terms of the different kind of sensors carried by the vehicles. One of the vehicles, the autonomous helicopter MARVIN of the Technical University of Berlin (TUB) (Remuss *et al.*, 2002) carries a fire sensor, which is a photodetector adjusted to respond to ultraviolet radiations characteristic of fire emission. The sensor gives a scalar measurement proportional to the radiation received. These raw values are thresholded obtaining a binary value that indicates if there is fire within the field of view of the sensor or not.

The helicopter HELIV (Ollero *et al.*, 2003) carries on board cameras of different modalities (infrared and visual). A fire segmentation algorithm is applied over the images before data fusion. Using the algorithm, both kind of images, infrared and visual, are transformed into binary images containing pixels classified as fire and pixels classified as not fire. These algorithms are not described in this paper. In (Martínez-de-Dios and Ollero, 2004) and (Phillips *et al.*, 2002) the algorithms for segmentation on IR and visual images respectively are presented. Figure 2 shows one infrared image as obtained by one of the vehicles.

Fig. 2. One infrared image of a scene with a fire.

Table 1. Preprocessed data characteristics

	Fire sensor	IR	Visual
P_D	95%	100%	90%
P_F	5%	10%	3%

As it will be seen, the Bayesian approach requires to characterize each sensor by its likelihood function, which mainly depends on the probabilities P_D of detection and P_F of false positive outputs. For the case of the fire sensor, this probabilities depend on the threshold selected. A higher threshold gives lower values of P_F but reduces the detection capabilities (P_D). The operating curve relating these values has been obtained using data from actual experiments with fire.

The image segmentation algorithms have also been analyzed with a large set of images to determine the values of P_D and P_F. Table 1 shows the values for the algorithms used for fire segmentation in visual and infrared images.

The sensors considered have different localization characteristics (that is, how much information a sensor provides about where a fire is). In the case of the fire sensor, the localization characteristics are poor, because it only provides a statement indicating the presence or absence of fire within the field of view of the sensor. In the case of the cameras, the localization capabilities are better, because cameras provides bearing measures. In the next section, a more detailed perception model of the sensors will be presented.

3. GRID-BASED COOPERATIVE ALARM DETECTION AND LOCALIZATION

This section presents the algorithm used for cooperative fire detection and localization. A digital elevation map is assumed to be available (which could be provided by other UAV (Hygounenc *et al.*, 2004). The 3D terrain surface is discretized using a 2D grid. Each cell i of the grid has a 3D associated position $\mathbf{x}_i$ and a probability $p(h_i)$ of containing fire. That is, each cell has associated a Bernoulli binary random variable, h_i. We denote by h_i the fact that there is fire at cell i and by $\bar{h}_i$ the fact that there is no fire at cell i, so that $p(h_i) = 1 - p(\bar{h}_i)$.

3.1 Generic equations of the evolution of the grid

The cells of the grid are evolved using a prediction-update cycle. Let $\mathbf{S}^{k+1} = \{\mathbf{S}_0, \ldots, \mathbf{S}_{k+1}\}$ be the set of all data gathered up to time $k+1$. The objective is to estimate, at time $k+1$, the posterior $p(h_{i,k+1}|\mathbf{S}^{k+1})$ for all the cells of the grid, that is, the probability of having fire at each cell i at time $k+1$, conditioned on the data. These data consists of fire sensor readings or segmented images.

This posterior probability can be written as:

$$p(h_{i,k+1}|\mathbf{S}^{k+1}) = p(h_{i,k+1}|\mathbf{S}_{k+1}, \mathbf{S}^k) \quad (1)$$

By the Bayes rule:

$$p(h_{i,k+1}|\mathbf{S}_{k+1}, \mathbf{S}^k) = \frac{p(\mathbf{S}_{k+1}|h_{i,k+1}, \mathbf{S}^k)p(h_{i,k+1}|\mathbf{S}^k)}{\eta} \quad (2)$$

where

$$\begin{aligned}\eta = p(\mathbf{S}_{k+1}|h_{i,k+1}, \mathbf{S}^k)p(h_{i,k+1}|\mathbf{S}^k) + \\ + p(\mathbf{S}_{k+1}|\bar{h}_{i,k+1}, \mathbf{S}^k)p(\bar{h}_{i,k+1}|\mathbf{S}^k)\end{aligned} \quad (3)$$

and $p(\bar{h}_{i,k+1}|\mathbf{S}^k) = 1 - p(h_{i,k+1}|\mathbf{S}^k)$ It is assumed that the measures at different time instants are independent, so that

$$p(\mathbf{S}_{k+1}|h_{i,k+1}, \mathbf{S}^k) = p(\mathbf{S}_{k+1}|h_{i,k+1}) \quad (4)$$

and the same applies for $p(\mathbf{S}_{k+1}|\bar{h}_{i,k+1}, \mathbf{S}^k)$. The term $p(h_{i,k+1}|\mathbf{S}^k)$ is computed from the information we have at time k, $p(h_{i,k}|\mathbf{S}^k)$ using equation 5:

$$p(h_{i,k+1}|\mathbf{S}^k) = \sum_j p(h_{i,k+1}|h_{j,k})p(h_{j,k}|\mathbf{S}^k) \quad (5)$$

where $p(h_{i,k+1}|h_{j,k})$ is the transition probability, that relates the probability of having fire at cell i if there is a fire at cell j the previous time instant. Thus, we state the dependency of $h_{i,k+1}$ on the full previous grid, and not only in the state of the cell $h_{i,k}$. The transition probability $p(h_{i,k+1}|h_{j,k})$ can take into account the neighbor relations between cells. This motion model depends on the application. For the fire application, and if nothing is known in advance (for example, the wind direction, which could be included in the model), this model consists of a smoothing of the probabilities in the grid, with equal probability of the fire propagating in all directions. Also, the slope of the terrain could be taken into account in the transition model.

So, if no new data are available, the information up to time $k+1$ is given by the prediction equation 5. Each time new data arrive from a vehicle of the fleet, the information is updated using equation 3.

The term $p(\mathbf{S}_{k+1}|h_{i,k+1})$ is the measurement model, the *likelihood* function. It indicates the probability of having data $\mathbf{S}_{k+1}$ considering that there is fire in cell i at time $k+1$. The data $\mathbf{S}_{k+1}$ consist of all the data gathered by the vehicles of the fleet at time $k+1$. The measurements by the different sensors are considered to be independent, and thus

$$p(\mathbf{S}_{k+1}|h_{i,k+1}) = \prod_j p(\mathbf{S}_{j,k+1}|h_{i,k+1}) \quad (6)$$

being j and index over all the sensors that provide data at time $k+1$.

The different terms in equation 6 will take into account the position of the sensors respect to the map and the geometric characteristics of the distinct sensors. The latter are obtained through calibration, while the former will be provided by the vehicles. For a correct update of the grid, it is very important to take into account the uncertainties in the position measurements.

At time $k+1$, for each sensor j, the hardware on board the UAVs provide an estimation of the position $\mathbf{t}_{j,k+1}$ and orientation of the sensor $\mathbf{R}_{j,k+1}$ in a global coordinate frame. We will denote this attitude data by $\mathbf{q}_{j,k+1}$. Each vehicle also provides an estimation of the errors on these quantities up the second order (the covariance matrix of these errors). The errors on the position data are taken into account when computing the likelihood. Thus, each factor in equation 6 becomes (the time index is removed from now on, unless necessary):

$$p(\mathbf{S}_j|h_i) = \int p(\mathbf{S}_j|h_i, \mathbf{q}_j)p(\mathbf{q}_j)d\mathbf{q}_j \quad (7)$$

Equivalent equations to 6 and 7 are used to compute $p(\mathbf{S}_j|\bar{h}_i)$.

3.2 Measurement equation for the fire sensor

After the preprocessing step, the sensor provides a binary decision stating if there is fire within its field of view or not. The field of view of the sensor is characterized by two aperture angles (vertical and horizontal) and a maximum range.

The model $p(\mathbf{S}_j|h_i, \mathbf{q}_j)$ is defined by the probabilities $P_{D,j}$ and $P_{F,j}$ of Table 1. These probabilities are modified depending mainly on the relative position of the cell i, $\mathbf{x}_i$, respect to the position and orientation of the sensor ($\mathbf{q}_j$). Thus:

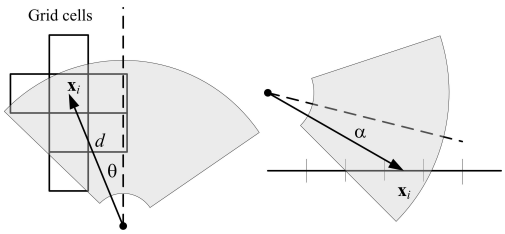

Fig. 3. Scheme of the fire sensor measurement model

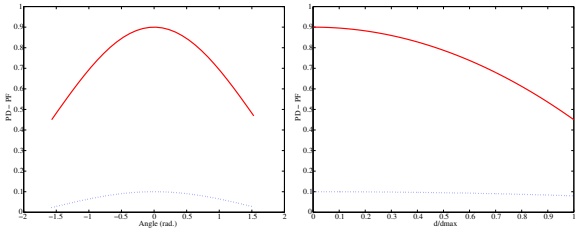

Fig. 4. Plots of equations 8 and 9. Left, angular component, right, distance component. Solid, P_D, dotted, P_F

$$P_{D,j}(\mathbf{x}_i, \mathbf{q}_j) = P_{D,j} - w_{D,j}(d_{ij}^2, \theta_{ij}, \alpha_{ij}) \quad (8)$$

$$P_{F,j}(\mathbf{x}_i, \mathbf{q}_j) = P_{F,j} - w_{F,j}(d_{ij}^2, \theta_{ij}, \alpha_{ij}) \quad (9)$$

where $w_{D,j}$ and $w_{F,j}$ are functions that decrease the values of $P_{D,j}$ and $P_{F,j}$ with the distance between cell i and sensor j, d_{ij}, and the angles that form cell i respect to the sensor j heading, $\theta_{i,j}$ and $\alpha_{i,j}$ (see Figure 3). Figure 4 shows a plot of these functions.

If the sensor detects fire, then the model is:

$$p(\mathbf{S}_j|h_i, \mathbf{q}_j) = P_{D,j}(\mathbf{x}_i, \mathbf{q}_j) \quad (10)$$

$$p(\mathbf{S}_j|\bar{h}_i, \mathbf{q}_j) = P_{F,j}(\mathbf{x}_i, \mathbf{q}_j) \quad (11)$$

If the sensor does not detect fire, then the model becomes:

$$p(\mathbf{S}_j|h_i, \mathbf{q}_j) = 1 - P_{D,j}(\mathbf{x}_i, \mathbf{q}_j) \quad (12)$$

$$p(\mathbf{S}_j|\bar{h}_i, \mathbf{q}_j) = 1 - P_{F,j}(\mathbf{x}_i, \mathbf{q}_j) \quad (13)$$

The evaluation of equation 7 can be done drawing samples from $p(\mathbf{q}_j)$. The main effect of equation 7 applies over the boundary of the field of view. However, in the particular case of the experiments presented, the UAV that carries the fire sensor has very good positioning capabilities, and then the effect of the uncertainties in $\mathbf{q}_j$ are neglected.

3.3 Measurement equation for the cameras

As a result of the preprocessing step, the data provided by the cameras are binary images in which true pixels indicate presence of fire, regardless the modality of the cameras.

The measurement function of the camera considers the pin-hole projection model. Each cell has a position associated, $\mathbf{x}_i$, and the center of the cell will correspond to a pixel $\mathbf{m}_{j,i}$ on the image plane of camera j (if it is within the field of view of the camera). If $\mathbf{x}_i$ and $\mathbf{m}_{j,i}$ are in homogeneous coordinates, the position of the pixel is given by

$$s\mathbf{m}_{j,i}^T = \mathbf{A}_j[\mathbf{R}_j\mathbf{t}_j]\mathbf{x}_i = \mathbf{f}(\mathbf{q}_j, \mathbf{x}_i) \quad (14)$$

where $\mathbf{A}_j$ is the internal calibration matrix of camera j. This matrix is obtained for every camera using a calibration procedure. $\mathbf{R}_j$ and $\mathbf{t}_j$ are the rotation and translation that refers the camera coordinate system and the global reference frame, and are provided, as said before, by the hardware on board the UAV.

To compute the likelihood $p(\mathbf{S}_j|h_i)$, equation 7 should be integrated for all possible values of $\mathbf{q}_j$. And this should be done for all the cells of the grid that are within the field of view of the camera. In this case is very important to take into account the uncertainties in $\mathbf{q}_j$, because the camera provides much more information about the location of the fire.

The direct solution of equation 7 using Monte-Carlo like procedures is computationally hard. Instead of directly solving equation 7, the uncertainties in $\mathbf{q}_j$ are propagated into uncertainties on the pixel position $\mathbf{m}_{j,i}$ through the non-linear function $\mathbf{f}$. This is done using the Unscented Transform (Julier and Uhlmann, 1997) (and actually, also the uncertainties in the position $\mathbf{x}_i$ due to the resolution of the grid are taken into account).

Then, equation (7) becomes:

$$p(\mathbf{S}_j|h_i) = \sum_{\mathbf{m}} p(s_j|\mathbf{m}_{j,i})p(\mathbf{m}_{j,i}) \quad (15)$$

The term $p(s_j|\mathbf{m}_{j,i})$ corresponds to equation 10 if pixel $\mathbf{m}_{j,i}$ corresponds to a region segmented as fire, while if the pixel is classified as background, then the term is given by equation 12. The same approximation is used to compute $p(\mathbf{S}_j|\bar{h}_i)$.

For the cameras, the weighting functions $w_{D,j}$ and $w_{F,j}$ in equations 8 and 9 only depend on the distance of the cell to the camera d_{ij}, and not on the relative orientation angles.

3.4 Obtaining measures from the grid

Using the equations described above, the status of the grid is recursively estimated using the data the vehicles are providing.

From a Bayesian point of view, the grid represents all the information about the possible fire alarms

Fig. 5. A view of the scenario from MARVIN helicopter

at time $k+1$. However, in some applications, more specific measures are required. For instance, if a fleet is looking for fire alarms, a control center would expect the position of the potential fire alarm detected, in order to plan a new mission, sending new vehicles to confirm the alarm. Also, we will use this value to compare it with the position of the fire recorded with GPS for validation purposes.

This can be accomplished in various ways. In this case, the set of cells of the grid with probabilities over a given threshold is obtained every T seconds. An alarm is raised for each set R of connected cells over this threshold. The position of the alarm is computed as the weighted geometric mean of the positions of the cells.

$$\mu_R = \frac{\sum_{i \subset R} \mathbf{x}_i p(h_i|\mathbf{S})}{\sum_{i \subset R} p(h_i|\mathbf{S})} \tag{16}$$

Also, it can be obtained an estimation of the uncertainty on the computed position from the second order moments of the region R.

4. EXPERIMENTAL RESULTS

4.1 Description of the experiments

The techniques described has been tested during field experiments involving several heterogeneous UAVs, in the frame of the COMETS project (Ollero *et al.*, 2005). The cooperative perception functions have a role in a more general mission of fire searching and confirmation, that also involves multi-robot path planning, coordination and other aspects not covered in this paper.

Figure 5 shows the scenario of the experiments as seen from autonomous helicopter MARVIN. During the experiments, a fire will be set up within the scenario. The scenario considered is a square of side-length of 400 meters approximately. The controlled fires used in the fire detection tests are originated by the burning of small shrubs. The fire position is previously recorded using a GPS receiver, as ground truth.

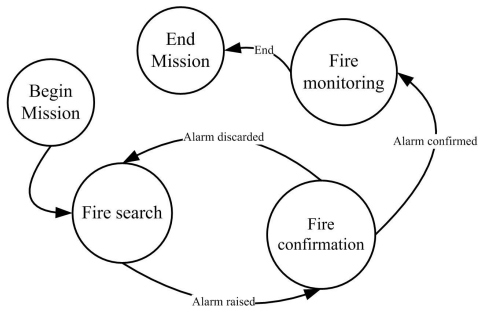

Fig. 6. General scheme of the mission considered.

A grid with resolution of 1 meter is defined over the scenario. The terrain is mostly planar, whose altitude is known. However, the method could be also used with any kind of terrain.

In the experiment presented, two UAVs, MARVIN and HELIV, are considered, one carrying a fire sensor and the other carrying an infrared camera. In the experiment, first MARVIN is sent, looking for potential fire alarms using the fire sensor. Then, if a possible fire alarm is raised from the grid, HELIV is sent over the position and both vehicles cooperate to confirm the alarm and to obtain the position of the alarm more precisely. If the alarm is confirmed, the mission continues initiating a monitoring phase not described here. Figure 6 shows a scheme of this mission.

4.2 Experimental results

Figure 7 shows the evolution of the grid in several phases of the experiment. The first image shows the status of the grid after MARVIN has flown over a place with no fire, using only the fire sensor. The second image shows how MARVIN produces two big high probability blobs on the grid, one due to a false alarm and other due to the actual alarm. Two alarms are generated and HELIV takes off and uses its IR camera over the zone of the possible alarms. The third image shows how after several images and fire sensor data are integrated, the high probability region is constrained to a smaller region, which includes the actual position of the fire.

Figure 8 shows the evolution of the position of the high probability regions computed using equation 16 compared to the actual fire position. It also shows the estimation on the uncertainty on the computed position.

Regarding the implementation issues, the grid fusion part of the algorithm is run in a centralized node. However, the preprocessing part (that is, the segmentation of the images and sensor preprocessing) is performed distributively, and each vehicle sends to the fusion algorithm the preprocessed data. This way, the bandwidth required to transmit the data is drastically reduced.

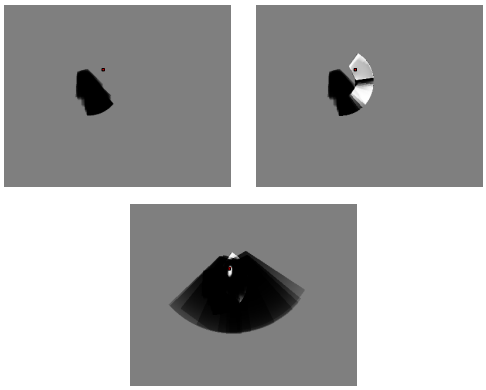

Fig. 7. The status of the grid at three moments during the mission. The filled square represents the actual position of the fire.

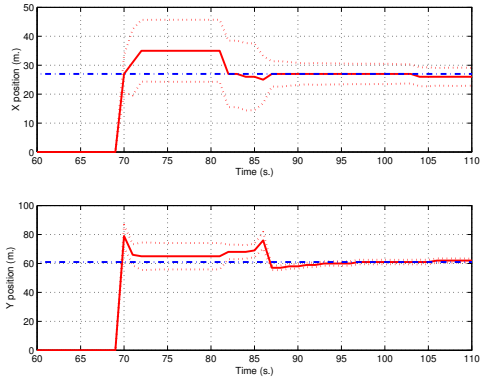

Fig. 8. Estimated mean position of one of the high probability regions. Dotted: estimated variances. Dash-dotted: actual fire position.

5. CONCLUSIONS AND FUTURE TRENDS

The paper shows how several different sensors can be integrated employing a probabilistic representation and a grid. It is assumed that the UAV are able to provide their positions in a global frame (in the experiments, GPS and compass are used to compute this global frame). For the proper working of the algorithm, it is very important to take into account the uncertainties in the UAV localization while updating the grid. The algorithm is tested in field conditions, and experimental results of actual flights with small controlled fires are presented.

A fully distributed version of the algorithm can be devised. Each vehicle could maintain and update a local grid, and include information from other robots of the fleet that can be broadcasted using the network established.

Also, this algorithm can be considered within a multi-UAV planning framework. In the COMETS project, the results from the detection functions are used to launch replanning in the mission. However, the grid itself provides more information, and can be used for intelligent path planning for exploration and other applications.

6. ACKNOWLEDGEMENTS

The authors thank the cooperation of the partners of the COMETS project, especially the members of the Technical University of Berlin, the Laboratoire d'Analyse et d'Architecture des Systémes (Toulouse, France) and ADAI from University of Coimbra (Portugal) for their participation in the COMETS experiments.

REFERENCES

Hygounenc, E., I-K. Jung, P. Soueres and S. Lacroix (2004). The Autonomous Blimp Project of LAAS-CNRS: Achievements in Flight Control and Terrain Mapping. *The International Journal of Robotics Research* **23**(4-5), 473–511.

Julier, S. and J. Uhlmann (1997). A new extension of the kalman filter to nonlinear systems. In: *Proceedings of the 11th Int. Symp. on Aerospace/Defence Sensing, Simulation and Controls.*

Martínez-de-Dios, J.R. and A. Ollero (2004). A multiresolution threshold selection method based on training. *Lecture Notes in Computer Science* **3211**, 90–97.

Ollero, A., J. Alcázar, F. Cuesta, F. López-Pichaco and C. Nogales (2003). Helicopter teleoperation for aerial monitoring in the COMETS multi-UAV system. In: *3rd IARP Workshop on Service, Assistive and Personal Robots.*

Ollero, A., S. Lacroix, L. Merino, J. Gancet, J. Wiklund, V. Remuss, I. Veiga, L. G. Gutierrez, D. X. Viegas, M. A.Gonzalez, A. Mallet, R. Alami, R. Chatila, G. Hommel, F. J. Colmenero, B. Arrue, J. Ferruz, J. R. Martinez and F. Caballero (2005). Multiple eyes in the sky: Architecture and perception issues in the COMETS unmanned air vehicles project. *IEEE Robotics and Automation Magazine* **12**(2), 46–57.

Phillips, W., M. Shah and N. da Vitoria Lobo (2002). Flame recognition in video. *Pattern Recogn. Lett.* **23**(1-3), 319–327.

Remuss, V., M. Musial and G. Hommel (2002). Marvin - an autonomous flying robot-bases on mass market. In: *International Conference on Intelligent Robots and Systems, IROS. Proceedings of the Workshop WS6 Aerial Robotics.* IEEE/RSJ. pp. 23–28.

Stepan, P., M. Kulich and L. Preucil (2005). Robust data fusion with occupancy grid. *IEEE Transactions on Systems, Man and Cybernetics, Part C* **35**(1), 106–115.

Thrun, S. (2001). A probabilistic online mapping algorithm for teams of mobile robots. *International Journal of Robotics Research* **20**(5), 335–363.